Front. Environ. Sci. Eng. 2014, 8(2): 162–168
DOI 10.1007/s11783-013-0507-2

RESEARCH ARTICLE

CO_2 adsorption performance of ZIF-7 and its endurance in flue gas components

Jiangkun XIE, Naiqiang YAN (✉), Fei LIU, Zan QU, Shijian YANG, Ping LIU

School of Environmental Science and Engineering, Shanghai Jiao Tong University, Shanghai 200240, China

Abstract Porous ZIF-7 with the sodalite (SOD) cage structure (ZIF, Zeolitic imidazolate framework) were synthesized by the solvothermal method. Synthesized material was characterized by powder X-ray diffraction (PXRD), thermal gravity (TG), scanning electron microscopy (SEM) and N_2 adsorption analysis. ZIF-8 with the SOD structure and a little larger pore window was synthesized in a similar way and was characterized for comparisons. Thermal stability and structural stability of ZIF-7 were tested through PXRD analysis, and the capability of the material for CO_2 capture from simulated flue gas was investigated through physical adsorption method. The results showed that CO_2 adsorption capacity on ZIF-7 was about 48 $mL \cdot g^{-1}$ while the capacity on ZIF-8 was about 18 $mg \cdot g^{-1}$ (at 12°C and 0.98 P/P_0 relative pressure). Furthermore, the impact of flue gas components on adsorption capacity of ZIF-7 and the selectivity of CO_2 against N_2 on ZIF-7 was also investigated in this work.

Keywords ZIF-7, structural stability, CO_2 capture, thermal stability

1 Introduction

With the rapid development of modern industry and society, fossil fuel consumption increases dramatically year by year. One of the consequences is the increase of CO_2 concentration in the environment. According to the prediction of Intergovernmental Panel on Climate Change (IPCC), CO_2 ratio in the atmosphere will be up to 570 ppm by the year 2100, which will cause a rise of about 1.9°C of mean global temperature and an increase of 3.8 m of mean sea level [1]. Therefore, CO_2 capture has become a burning issue all over the world. Large power plants based on fossil fuel combustion contribute a lot in CO_2 emissions and CO_2 capture in these large point sources has attracted much more attentions [2]. To date, many technologies have been developed for CO_2 capture, such as amine absorption [3], cryogenic distillation [4] and so on. However, all these technologies have their intrinsic drawbacks, and the most fatal one is their high energy cost for regeneration or the achievement of extremely low temperature. Adsorption method could overcome this disadvantage, due to no phase transformation and no chemical bond formation in the operation process. Pressure swing adsorption (PSA, feed gas is compressed substantially higher than atmospheric pressure and adsorbed gas is recovered under atmospheric pressure) and vacuum swing adsorption (VSA, feed gas is slightly compressed and adsorbed gas is recovered by vacuum) have been applied as mature processes [5]. However, the process using PSA or VSA for CO_2 capture from flue gas is still under developing due to the lack of high performance sorbent for CO_2. Therefore, developing novel adsorbent with high performance for CO_2 is of great significance.

Recently, a novel class of porous materials named metal-organic frameworks (MOFs) has attracted more research interests [6–12]. But the fragile stability of this kind of material due to the instinct property of its organic ligand limited its application in harsh conditions. Interestingly, zeolitic imidazolate frameworks (ZIFs), a sub-family of MOFs, which consisted of metal tetrahedral and imidazolate (or its derivative) ligands, have been reported possessing relatively high thermal stability and chemical stability [13–15]. Among these materials, ZIF-8 should be the most famous one and have been studied extensively [16]. As its analog, ZIF-7 also has the open framework with sodalite (SOD) cage structure but relatively smaller pore windows (0.30 and 0.35 nm) [17,18]. Such smaller pore size may restrict the entry of N_2 molecule but allow the access of CO_2 molecule, therefore, high selectivity of CO_2 against N_2 on ZIF-7 is anticipated. Recently, some researches and patents have published the selective

Received December 29, 2011; accepted March 21, 2013

E-mail: nqyan@sjtu.edu.cn

separation of alkane from alkene, CO_2 from N_2, and hydrogen from hydrocarbons on ZIF-7 [19–22]. However, so far as we know, there is no study regarding on the influence of flue gas components on the structure stability and adsorption performance of ZIF-7 has been reported yet.

Herein, ZIF-7 crystals were synthesized and characterized. Its structure stability in flue gas components was tested by powder X-ray diffraction (PXRD) analysis, and its CO_2 adsorption capacity was determined before and after the treatment in flue gas components to investigate the influence of flue gas components on adsorption performance. As an analog, ZIF-8 was also synthesized and characterized for comparison.

2 Experimental sections

2.1 Synthesis and activation of the materials

ZIF-7 and ZIF-8 were synthesized by solvothermal method and activated according to published procedure [23] with little modification. Brief procedures are as follows:

ZIF-7: A solid mixture of zinc nitrate hexahydrate $Zn(NO_3)_2 \cdot 6H_2O$ (2 mmol, 0.595 g) and benzimidazole (H-PhIM) (2 mmol, 0.2365 g) was dissolved in 45 mL *N*,*N*-dimethylformamide (DMF) in a 50 mL vial. The vial was capped tightly and put into an oven, held at 130°C for 24 h, then cooled down to room temperature in the air. Mother liquor was decanted, and colorless cubic crystals of ZIF-7 were collected, washed with DMF (3 mL × 3) and methanol (3 mL × 3) sequentially, and then immersed in methanol overnight to exchange the solvent. Crystal particles were collected after being dried at 130°C.

ZIF-8: A solid mixture of zinc nitrate hexahydrate $Zn(NO_3)_2 \cdot 6H_2O$ (2 mmol, 0.595 g) and 2-methylimdazole (H-MeIM) (2 mmol, 0.1642 g) was dissolved in 45 mL DMF in a 50 mL vial. The vial was capped tightly and put into an oven, held at 130°C for 24 h, then cooled down to room temperature in the air. Mother liquor was decanted, and colorless cubic crystals of ZIF-8 were collected, washed with DMF (3 mL × 3) and methanol (3 mL × 3) sequentially, and then immersed in methanol overnight to exchange the solvent. Crystal particles were collected after being dried at 130°C.

All regents (Aladdin Chemistry Co., Ltd, China) were used as received (AR grade) without further purification.

2.2 Structure stability in air moisture

ZIF-7 crystal particles (100 mg) were enveloped in moist air (containing about 2.6% of water vapor, v/v) for 1, 3 and 5 d respectively, thereafter, PXRD patterns of each sample were collected to test whether the crystal structure had changed.

2.3 Structure stability in SO_2

ZIF-7 crystal particles (100 mg) were enveloped in SO_2/N_2 (v/*v*, 1/99) mixture for 1, 3 and 5 d respectively, thereafter, PXRD patterns of each sample were collected to test whether the crystal structure had changed.

2.4 Structural stability in NO

ZIF-7 crystal particles (100 mg) were enveloped in NO/N_2 (v/v, 1/99) mixture for 1, 3 and 5 d respectively, thereafter, PXRD patterns of each sample were collected to investigate whether the crystal structure had changed.

2.5 Structural stability in moist air/SO_2/NO mixture

ZIF-7 crystal particles (100 mg) were enveloped in SO_2/NO/moist air mixture (v/v/v, 1/1/98) for 5 d, thereafter, PXRD patterns of each sample were collected to investigate whether the crystal structure had changed.

2.6 Morphology characterization

Images of the ZIF-7 and ZIF-8 crystals were taken with a scanning electron microscope (Hitachi S-2150, Hitachi, Japan) after gold deposition.

2.7 Thermal gravimetric analysis

Thermal gravimetric analysis was performed on a Netzsch STA 409PC Instrument (Netzsch, German). Powder sample was weighed and heated in a corundum crucible from 30°C to 580°C at the heating rate of $5°C \cdot min^{-1}$ under highly pure N_2 atmosphere ($60 mL \cdot min^{-1}$), and the curve of weight loss over temperature was collected.

2.8 Specific surface area measurement

Brunauer-Emmett-Teller (BET) surface areas of ZIF-7 and ZIF-8 were measured by Quantachrome Nova 2200e Surface & Pore Size Analyzer (Quantachrome, America) using highly pure nitrogen as adsorbate. At first, certain mass of sample was activated under vacuum at 155°C for 3 h in activation chamber, and then the sample was transferred into the measurement room to collect multi-point BET data in a liquid nitrogen bath.

2.9 CO_2 adsorption measurement

CO_2 adsorption measurements were also performed on Quantachrome Nava 2200e Surface & Pore Size Analyzer by submerging the sample holder in an isothermal water bath (at 12°C). After the same activation procedure in BET measurement, adsorption isotherms of CO_2 were recorded using highly pure CO_2 as adsorbate.

2.10 Packed bed experiment

ZIF-7 particles were filled in a glass column to build a packed bed. CO_2/N_2 mixture (0.5 mL per dose) was intermittently driven through the column. The effluent was collected and injected into a chromatography to detect the concentration of CO_2 and N_2 after the packed bed. Thermal conductivity cell was used as the gas detector. After detection, the concentration of CO_2/N_2 was calculated based the peak area. The initial concentration of CO_2/N_2 in the mixture was 50/50 (v/v).

3 Results and discussion

First, the prepared ZIF-7 and ZIF-8 were analyzed by powder X-ray diffraction to identify whether the correct structure was obtained. As was shown in Fig. 1, both patterns matched well with published literatures [23,24], indicating ZIF-7 and ZIF-8 were successfully synthesized.

Generally, smaller size often leads to larger surface which could provide more active sites for interaction between adsorbent and adsorbate. To date, electron microscope has become a common tool for morphology characterization of the material. Herein, images of ZIF-7 and ZIF-8 were taken with a scanning electron microscope after gold deposition. As illustrated in Fig. 2, both ZIF-7 and ZIF-8 aggregated together and formed particles with the diameter of about 1 to 20 μm and displayed their good crystallization which was corroborated by powder X-ray diffraction patterns.

To be applied in flue gas condition, materials should be able to keep its structure at flue gas temperature. Thermogravimetric curve for ZIF-7 and ZIF-8 were taken to test their thermal stability. As shown in Fig. 3, about 15% weight loss of ZIF-7 could be observed from the beginning temperature to 250°C that could be attributed to the removal of solvent molecules adsorbed on the surface. After then, a plateau was observed from 250°C to 550°C, indicating the maintenance of the structure within this temperature range. Similarly, ZIF-8 lost about 17% of its weight as the temperature increased

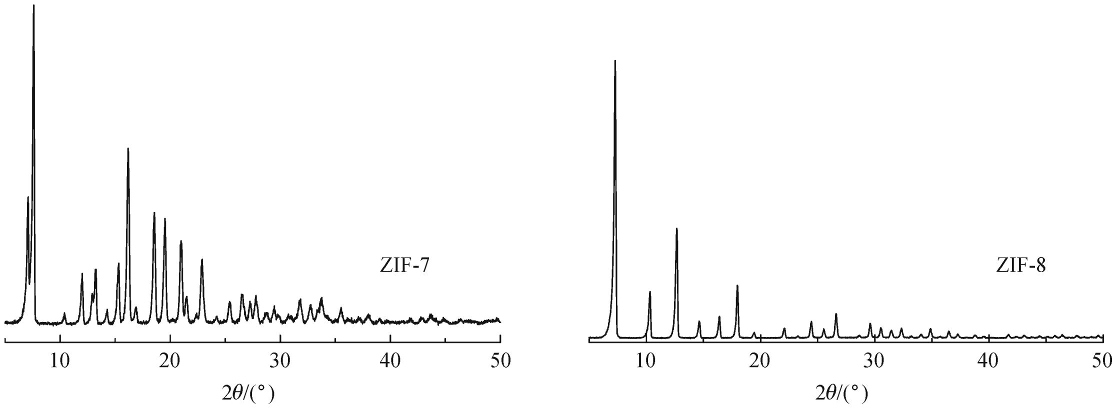

Fig. 1 PXRD patterns of ZIF-7 and ZIF-8

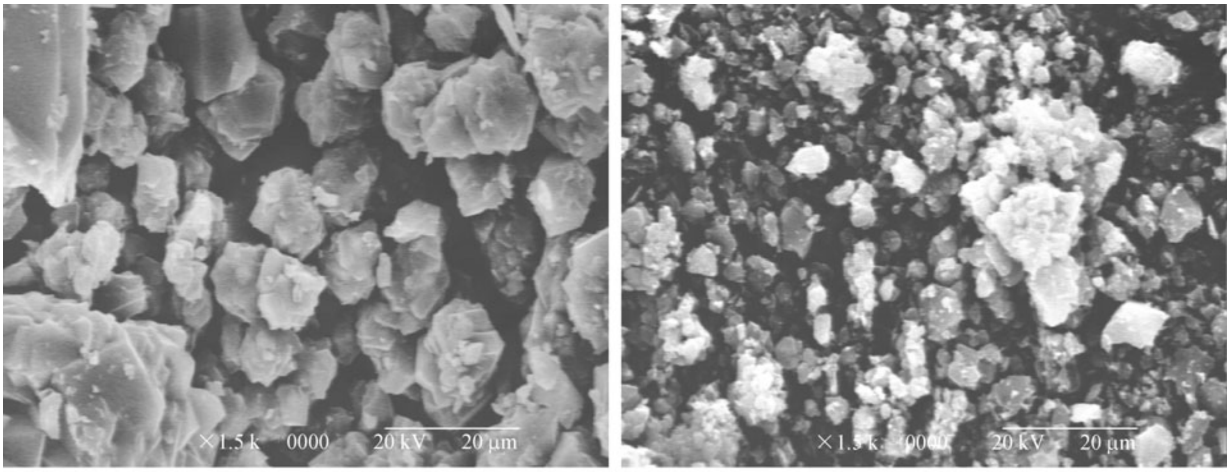

(a)

(b)

Fig. 2 SEM images of ZIF-7 (a) and ZIF-8 (b)

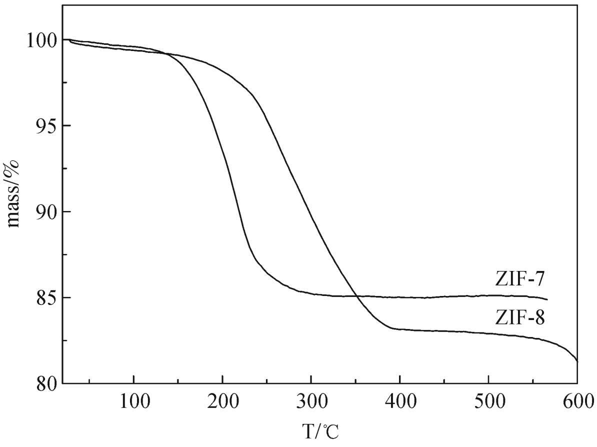

Fig. 3 TG curves of ZIF-7 and ZIF-8

from 25°C to 380°C, due to the removal of the solvent in its pores. Taking common flue gas temperature into consideration, both ZIF-7 and ZIF-8 would not collapse in common flue gas.

Not only thermal stability but also chemical stability is very important for the material. In this study, the stability of ZIF-7 in moist air, SO_2 or NO was tested by PXRD analysis. As shown in Fig. 4, after ZIF-7 sample was exposed to moist air (containing about 2.6% of water vapor, v/v) at room temperature for 1, 3 and 5 d, no significant peak change could be observed from PXRD patterns, which indicated framework of ZIF-7 could maintain well in the presence of moist air after 5 d.

Similarly, in order to determine the stability of the material in the presence of SO_2, the crystals were enveloped and kept in SO_2/N_2 (v/v, 1/99) mixture at room temperature for 1, 3 and 5 d, respectively. As shown in Fig. 5, PXRD patterns of ZIF-7 were almost the same before and after being exposed to SO_2/N_2 mixture after 5 d.

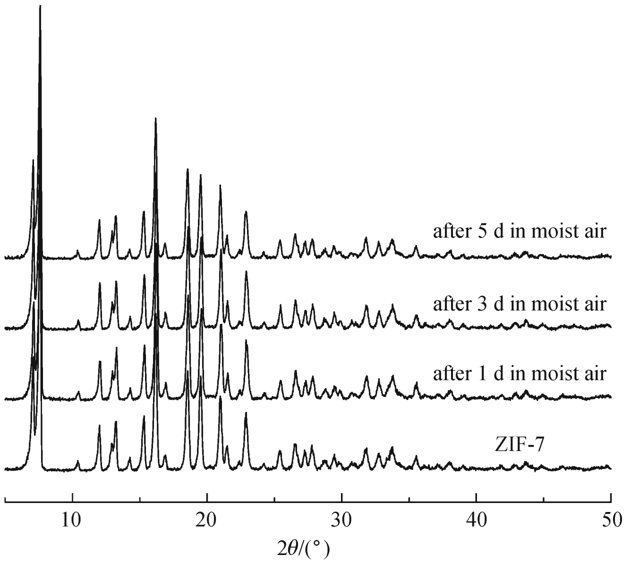

Fig. 4 XRD patterns of ZIF-7 before and after treatment in moist air at room temperature for 1, 3 and 5 d

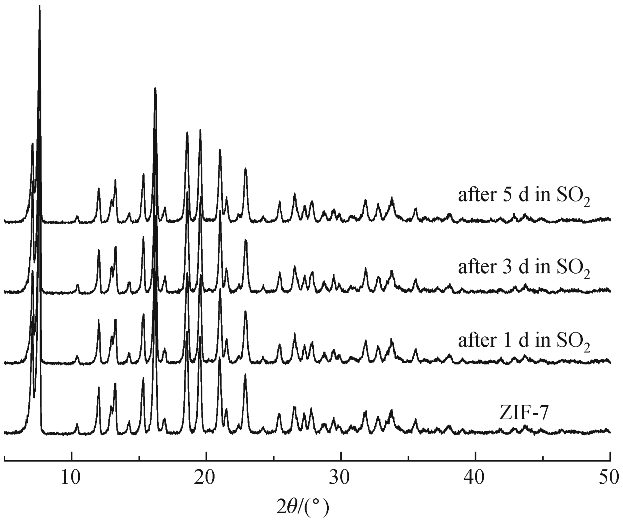

Fig. 5 XRD patterns of ZIF-7 before and after treatment in SO_2/N_2 mixture at room temperature for 1, 3 and 5 d

While testing the stability of ZIF-7 in NO which was also one common component in flue gas, there was still no changes observed from PXRD patterns before and after treatment at room temperature in NO/N_2 mixture for 1, 3 and 5 d (Fig. 6). This illustrated that crystal structure of ZIF-7 was stable in the presence of low concentration of NO.

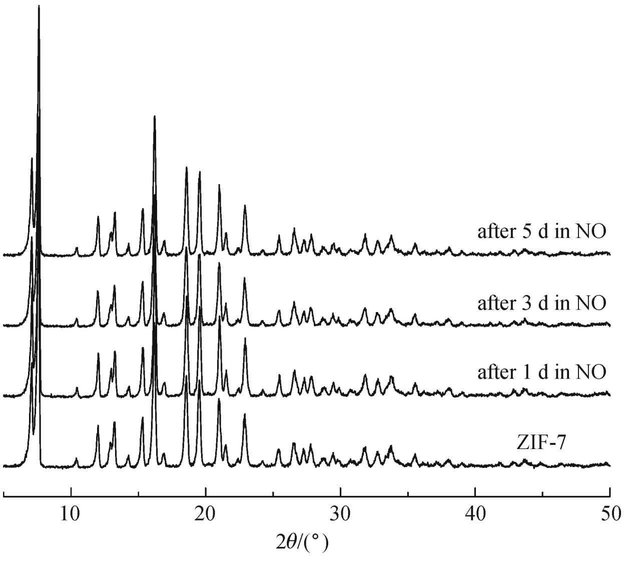

Fig. 6 XRD patterns of ZIF-7 before and after treatment in NO/N_2 mixture at room temperature for 1, 3 and 5 d

For applications in the flue gas condition, only considering the stability of the material in single component was not sufficient, its stability in their mixture should also be considered. PXRD analysis was employed to investigate the structure stability of ZIF-7 in the presence of common flue gas components. As shown in Fig. 7, after enveloping ZIF-7 sample in the mixture of SO_2, NO and moist air (v/v/v, 1/1/98) at room temperature for 5 d, no significant change could be observed in PXRD pattern comparing with fresh ZIF-7. The result demonstrated good chemical stability of ZIF-7 in flue gas components.

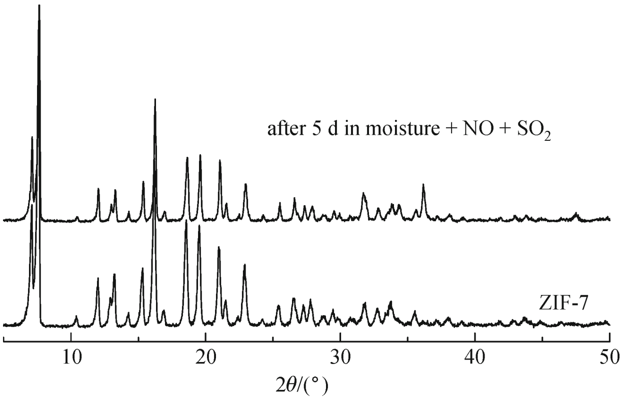

Fig. 7 XRD patterns of ZIF-7 before and after treatment in moist air/NO/SO_2 mixture at room temperature for 5 d

In addition to stability, high CO_2 capacity was an indispensable property for the adsorbent. Herein, both the N_2 and CO_2 adsorption behaviors on ZIF-7 and ZIF-8 were investigated using a Quantachrome Nova 2200e Surface & Pore Size Analyzer. According to N_2 and CO_2 adsorption results shown in Fig. 8, ZIF-7 and ZIF-8 displayed different types of adsorption isotherms. The BET surface area of ZIF-7 was only about $20\,m^2\cdot g^{-1}$ while ZIF-8 was about $1280\,m^2\cdot g^{-1}$, but the CO_2 capacity of ZIF-7 (about $48\,mL\cdot g^{-1}$ at 0.98 P/P_0 and 12°C) was much higher than that of ZIF-8 (about $18\,mL\cdot g^{-1}$ at 0.98 P/P_0 and 12°C). This could be attributed to its relatively small pore diameter (0.35 nm of distorted hexagonal windows) [17], which restricted the entry of N_2 molecule (0.36–0.38 nm of kinetic diameter) but didn't inhibit the entry of relatively small CO_2 molecule (0.33 nm of kinetic diameter) [24]. CO_2 capacity displayed a significant increase on ZIF-7 when the relative pressure reached higher than 0.2 P/P_0. This could be explained by so-called gate-opening effect [20].

Moreover, for industrial applications, the influence of flue gas components such as SO_2 and NO on CO_2 capacity of the adsorbent should also be considered. In this work, samples after pre-treated in moist air, SO_2 and NO for 5 d were collected to measure their adsorption capacity. By comparing Figs. 9(a)–(c) with Fig. 8(b), it could be concluded that the CO_2 capacity (at 0.98 P/P_0, 12°C) before and after treatment in moist air, SO_2 and NO were almost the same. This illustrated that pre-treatment in flue gas components would not affect CO_2 capacity of ZIF-7. Furthermore, although hysteresis was displayed on desorption curve in Fig. 9, the adsorption and desorption curve still closed, indicating the material could be regenerated through vacuuming. According to adsorption and desorption curves, we could also find that the adsorption amount of CO_2 increased with the increase of relative pressure, and a drastic increase appeared at 0.2 P/P_0 after which the curve became flat. It meant that a higher CO_2 capacity could be achieved at low relative pressure on ZIF-7 which lowered the energy requirement for pressurizing flue gas. The regenerable ability and high CO_2 capacity of ZIF-7 at low relative pressure enunciated its application potential for CO_2 separation by adsorption method.

To study the selectivity of CO_2 against N_2 on ZIF-7, a ZIF-7 packed bed was built and CO_2/N_2 (50/50, v/v) mixture (0.5 mL per dose) was intermittently driven through the column. The gaseous effluent was collected and injected into a chromatography to detect the

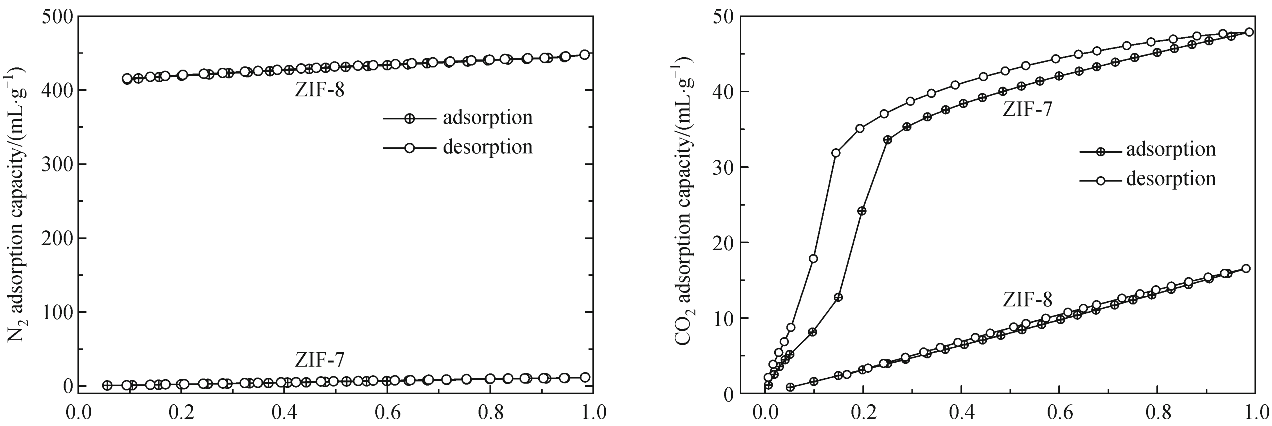

(a) (b)

Fig. 8 Adsorption and desorption curve of N_2 (a) and CO_2 (b) on ZIF-7 and ZIF-8 at 12°C

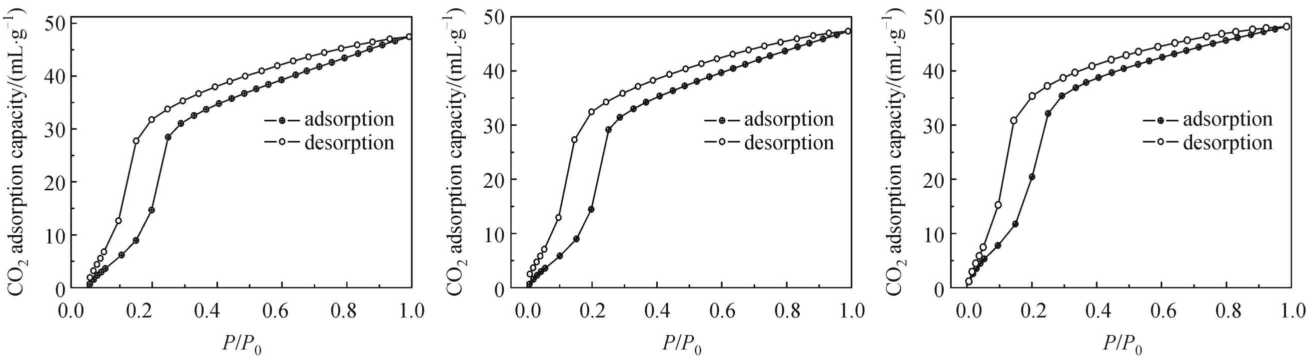

(a) (b) (c)

Fig. 9 Adsorption and desorption curves of CO_2 on ZIF-7 after treatment in moist air (a), SO_2 (b) and NO (c) at 12°C for 5 d

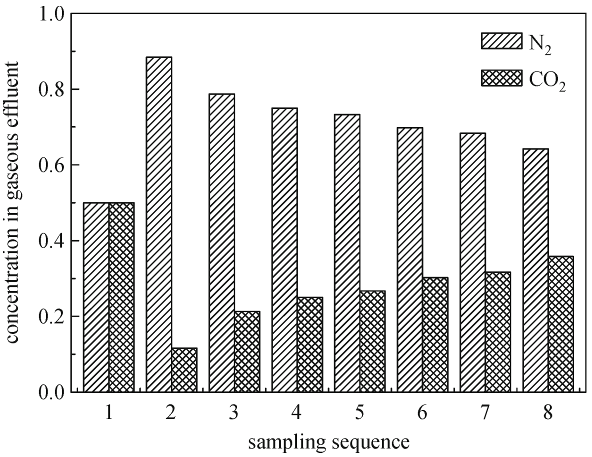

Fig. 10 CO_2 and N_2 concentration in gaseous effluent passing through ZIF-7 packed bed at room temperature (The abscissa 0 denotes the initial gaseous mixture, abscissa 1-7 denote the 1-7th gaseous effluent)

concentration of CO_2/N_2 in the effluent. Peak areas was recorded and translated into concentrations. Relations between component concentration and sampling sequence were illustrated in Fig. 10. At the beginning, CO_2/N_2 (v/v, 50/50) mixture was directly injected in the chromatography to get a benchmark (see abscissa-0 in Fig. 10), after the mixture was driven through ZIF-7 packed bed, CO_2 concentration decreased significantly (see abscissa-1 in Fig. 10) in the gaseous effluent accompanying with an increase of N_2 concentration. This result indicated CO_2 was preferably adsorbed on ZIF-7 against N_2. With the next dose of the mixed gas, the bed tended to break through gradually (see abscissa 2–7 in Fig. 10). It meant that ZIF-7 had a high CO_2 selectivity against N_2 before the breakthrough of packed bed.

4 Conclusions

Well crystalline ZIF-7 and ZIF-8 porous materials were synthesized through solvothermal method. The thermal stability and chemical stability in flue gas component were illustrated by PXRD analysis. ZIF-7 had a high CO_2 adsorption capacity (about 48 $mL \cdot g^{-1}$ at 0.98 P/P_0 and 12°C) comparing with its analog ZIF-8 (about 18 $mL \cdot g^{-1}$ at 0.98 P/P_0 and 12°C). Furthermore, the adsorption capacity of CO_2 on ZIF-7 was not significantly influenced by the presence of flue gas components. The adsorption selectivity of CO_2 on ZIF-7 against N_2 was also demonstrated by packed bed experiment. In conclusion, with its high thermal stability, excellent stability in flue gas component, high CO_2 adsorption capacity and high CO_2 selectivity against N_2, ZIF-7 has the potential to be employed as the suitable material for CO_2 capture from gaseous mixtures.

Acknowledgements Dr. Yongfu Guo, Yongpeng Ma, Bing Pei, Wenqi Zhang, Haomiao Xu, Kaihua Li and Wanmiao Chen were thanked for helpful discussions.

References

1. Stewart C, Hessami M A. A study of methods of carbon dioxide capture and sequestration-the sustainability of a photosynthetic bioreactor approach. Energy Conversion and Management, 2005, 46 (3): 403–420
2. D'Alessandro D M, Smit B, Long J R. Carbon dioxide capture: prospects for new materials. Angewandte Chemie International Edition, 2010, 49(35): 6058–6082
3. Gray M L, Soong Y, Champagne K J, Pennline H, Baltrus J P, Stevens R W Jr, Khatri R, Chuang S S C, Filburn T. Improved immobilized carbon dioxide capture sorbents. Fuel Processing Technology, 2005, 86(14–15): 1449–1455
4. Hart A, Gnanendran N. Cryogenic CO_2 capture in natural gas. Energy Procedia, 2009, 1(1): 697–706
5. Zhang J, Webley P A, Xiao P. Effect of process parameters on power requirements of vacuum swing adsorption technology for CO_2 capture from flue gas. Energy Conversion and Management, 2008, 49(2): 346–356
6. Britt D, Furukawa H, Wang B, Glover T G, Yaghi O M. Highly efficient separation of carbon dioxide by a metal-organic framework

replete with open metal sites. Proceedings of the National Academy of Sciences of the United States of America, 2009, 106(49): 20637–20640

7. Britt D, Tranchemontagne D, Yaghi O M. Metal-organic frameworks with high capacity and selectivity for harmful gases. Proceedings of the National Academy of Sciences of the United States of America, 2008, 105(33): 11623–11627
8. Millward A R, Yaghi O M. Metal-organic frameworks with exceptionally high capacity for storage of carbon dioxide at room temperature. Journal of the American Chemical Society, 2005, 127 (51): 17998–17999
9. Sudik A C, Millward A R, Ockwig N W, Cote A P, Kim J, Yaghi O M. Design, synthesis, structure, and gas (N_2, Ar, CO_2, CH_4, and H_2) sorption properties of porous metal-organic tetrahedral and heterocuboidal polyhedra. Journal of the American Chemical Society, 2005, 127(19): 7110–7118
10. Caskey S R, Wong-Foy A G, Matzger A J. Dramatic tuning of carbon dioxide uptake via metal substitution in a coordination polymer with cylindrical pores. Journal of the American Chemical Society, 2008, 130(33): 10870–10871
11. Liang Z J, Marshall M, Chaffee A L. CO_2 Adsorption-based separation by metal organic framework (Cu-BTC) versus zeolite (13X). Energy & Fuels, 2009, 23(5): 2785–2789
12. Yazaydın A Ö, Benin A I, Faheem S A, Jakubczak P, Low J J, Willis R R, Snurr R Q. Enhanced CO_2 adsorption in metal-organic frameworks via occupation of open-metal sites by coordinated water molecules. Chemistry of Materials, 2009, 21(8): 1425–1430
13. Phan A, Doonan C J, Uribe-Romo F J, Knobler C B, O’Keeffe M, Yaghi O M. Synthesis, structure, and carbon dioxide capture properties of zeolitic imidazolate frameworks. Accounts of Chemical Research, 2010, 43(1): 58–67
14. Yazaydın A Ö, Snurr R Q, Park T, Koh K, Liu J, LeVan M D, Benin A I, Jakubczak P, Lanuza M, Galloway D B, Low J J, Willis R R. Screening of metal-organic frameworks for carbon dioxide capture from flue gas using a combined experimental and modeling approach. Journal of the American Chemical Society, 2009, 131 (51): 18198–18199
15. Banerjee R, Phan A, Wang B, Knobler C, Furukawa H, O’Keeffe M, Yaghi O M. High-throughput synthesis of zeolitic imidazolate frameworks and application to CO_2 capture. Science, 2008, 319 (5865): 939–943
16. Chang N, Gu Z Y, Yan X P. Zeolitic imidazolate framework-8 nanocrystal coated capillary for molecular sieving of branched alkanes from linear alkanes along with high-resolution chromatographic separation of linear alkanes. Journal of the American Chemical Society, 2010, 132(39): 13645–13647
17. Li Y S, Bux H, Feldhoff A, Li G L, Yang W S, Caro J. Controllable synthesis of metal-organic frameworks: from MOF nanorods to oriented MOF membranes. Advanced Materials (Deerfield Beach, Fla.), 2010, 22(30): 3322–3326
18. Li Y S, Liang F Y, Bux H G, Yang W S, Caro J. Zeolitic imidazolate framework ZIF-7 based molecular sieve membrane for hydrogen separation. Journal of Membrane Science, 2010, 354(1–2): 48–54
19. Gücüyener C, van den Bergh J, Gascon J, Kapteijn F. Ethane/Ethene separation turned on its head: selective ethane adsorption on the metal-organic framework ZIF-7 through a gate-opening mechanism. Journal of the American Chemical Society, 2010, 132(50): 17704–17706
20. van den Bergh J, Gücüyener C, Pidko E A, Hensen E J M, Gascon J, Kapteijn F. Understanding the anomalous alkane selectivity of ZIF-7 in the separation of light alkane/alkene mixtures. Chemistry (Weinheim an der Bergstrasse, Germany), 2011, 17(32): 8832–8840
21. Aguado S, Bergeret G, Titus M P, Moizan V, Nieto-Draghi C, Bats N, Farrusseng D. Guest-induced gate-opening of a zeolite imidazolate framework. New Journal of Chemistry, 2011, 35(3): 546–550
22. Kaye S S, Dailly A, Yaghi O M, Long J R. Impact of preparation and handling on the hydrogen storage properties of Zn_4O(1,4-benzenedicarboxylate)$_3$ (MOF-5). Journal of the American Chemical Society, 2007, 129(46): 14176–14177
23. Park K S, Ni Z, Cote A P, Choi J Y, Huang R D, Uribe-Romo F J, Chae H K, O'Keeffe M, Yaghi O M. Exceptional chemical and thermal stability of zeolitic imidazolate frameworks. Proceedings of the National Academy of Sciences of the United States of America, 2006, 103(27): 10186–10191
24. Li J R, Kuppler R J, Zhou H C. Selective gas adsorption and separation in metal-organic frameworks. Chemical Society Reviews, 2009, 38(5): 1477–1504